Environmental Earth Sciences (2022) 81:190
https://doi.org/10.1007/s12665-022-10305-z

THEMATIC ISSUE

The role of geological models and uncertainties in safety assessments

Merle Bjorge[1] · Phillip Kreye[1] · Elisa Heim[2] · Florian Wellmann[3,4] · Wolfram Rühaak[1]

Received: 23 June 2021 / Accepted: 19 February 2022 / Published online: 16 March 2022

Abstract
Safety assessments in nuclear waste management typically include the analysis of thermo-mechanical (TM)-coupled processes. The TM behavior of the host rock is, among other aspects, dependent on the prevalent geological geometry. This study aims to evaluate the impact of uncertainties in geometry on the TM rock behavior. It is one of the very first studies aiming to bring uncertainties of structural geological models and numerical simulations together. To analyze the influence of geological geometries, a simplified model of the region around the Mont Terri rock laboratory was created. A 3D structural geological model was set up and uncertainties of the lithological contacts were quantified by means of stochastic simulations, resulting in an ensemble of 89 model realizations. These realizations were transformed to a 2D numerical model. In this numerical model, TM simulations were computed over a simulation time of 500 years, employing the Finite Element Method. To simulate a heat source of nuclear waste, the lower edge of the model was set to 100 °C. The results of these simulations show mean temperature variations of 90.89 and 92.70 °C after 500 years, with a maximum stress varying between 0.02 and 0.16 MPa of elastic shear energy density and according mean cumulative displacements ranging from 30 to 38 cm. The presented results indicate that different model geometries and differences in material properties lead to noticeable variabilities of the TM behavior of claystone. However, in this case, these variabilities would not significantly affect the integrity of the rock.

Keywords Nuclear waste disposal · Safety assessments · Thermo-mechanical modeling · Uncertainties · 3D modeling

Introduction

Safety assessments present an important part for nuclear waste management (BGE 2020; SKB 2015; Nagra 2002). The safety assessments, along with the safety case, demonstrate that the safety requirements for the disposal of nuclear waste are fulfilled. One important aspect of the safety assessments is the evaluation of thermo-mechanical (TM) effects created by elevated temperatures in host rock and overburden. Important tools for the safety assessments are coupled numerical models, which allow the evaluation of these effects (Birkholzer et al. 2019; Rühaak et al. 2014, 2017). These numerical models generally incorporate geometrical information from 3D geological models to parameterize the simulations according to properties in major geological domains. However, this information about the geometry of the subsurface is not completely certain. Since this knowledge about the subsurface is based on different data, e.g., data from mapping, drillings or seismic explorations, it involves uncertainties due to resolution, measurement errors, etc. These uncertainties have been addressed in different studies by, e.g., Rühaak et al. (2015), Wellmann and Caumon (2018) or Wellmann et al. (2010). With a view to the disposal of nuclear waste, this leads to the following questions: How do uncertainties in geometry affect the respective TM behavior of the rock? Will these effects have an impact on the rock integrity

This article is part of a Topical Collection in Environmental Earth Sciences on Deep Geological Disposal, guest edited by Thomas Nagel, Wolfram Rühaak, Florian Amann, Guido Bracke, Stefan Buske, Julia Kowalski, Sönke Reiche, Thorsten Schäfer, Traugott Scheytt, Thorsten Stumpf, Holger Völzke, Florian Wellmann.

✉ Merle Bjorge
merle.bjorge@bge.de

1 Bundesgesellschaft für Endlagerung mbH (BGE), Peine, Germany

2 Applied Geophysics and Geothermal Energy, RWTH Aachen University, Aachen, Germany

3 Lehr- und Forschungsgebiet Computational Geoscience and Reservoir Engineering, RWTH Aachen University, Aachen, Germany

4 Aachen Institute for Advanced Study in Computational Engineering Science, RWTH Aachen University, Aachen, Germany

and therefore the safety of the system? Within the Swiss Sectoral Plan for Deep Geological Repositories, Nagra has performed computational cases in 1D considering different thicknesses of rock layers (Nagra 2014). However, uncertainties regarding geometry are not investigated in more detail (e.g., by considering higher dimensions or other geometrical aspects) and by now, the authors are not aware of any respective studies. Therefore, to investigate these questions, a workflow was established to study the effects of uncertainties of a 3D geological model on a respective 2D TM-coupled numerical model.

Methods

For the purpose of this study, a generic model was developed based on the Opalinus Clay in Mont Terri (Fig. 1). A 3D geological model of the Opalinus Clay was created and the uncertainties of the lithological contacts were statistically assessed, leading to multiple model realizations with thickness variations of the different lithological units. For each model realization, one TM numerical simulation was conducted. This simulation covered a time span of 500 years directly after the disposal of the nuclear waste and results included calculated stress, strain and temperature. The results of all simulations from all stochastic modeling realizations were then compared to obtain an insight on the variability and the impact of the uncertainties.

Set-up of the 3D geological model

For this study, a generic, simplified model of the Opalinus Clay around the Mont Terri Rock Laboratory was created. As input data, a geological map of the underground rock laboratory and orientation measurements (strike and dip measurements obtained from Bossart and Thury (2008)) were used (Fig. 1).

The Opalinus Clay in Mont Terri consists of three different facies, the shaly facies, the sandy facies and the carbonate-rich sandy facies (Bossart et al. 2017). However, for sake of simplicity only two facies, the sandy and the shaly facies, were implemented in this study. The carbonate-rich sandy facies was treated as part of the sandy facies and was parameterized accordingly. The 3D geological model was created with *GemPy*, an implicit geological modeling program (de la Varga et al. 2019). The final model covers an extent of about 230 m in *x*-direction, 310 m in *y*-direction and has a vertical extent of 100 m. A sketch of this model is displayed in Fig. 2. The model units of the sandy and shaly facies were assigned according to the corresponding parameters, which are shown in Table 1.

Assigning uncertainties and producing multiple model realizations

Two different types of uncertainty were assigned to the input data of the 3D geological model with the aim to produce multiple stochastic model realizations of the initial

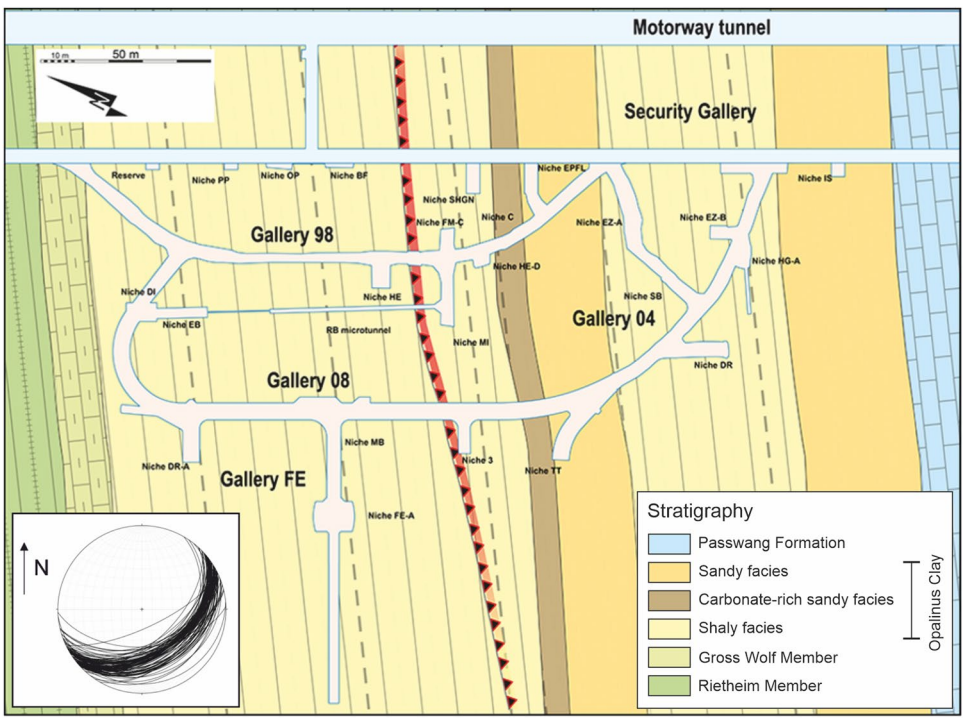

Fig. 1 Input data used fort the 3D geological model, including a geological map displaying the geological contacts and orientation measurements (modified from Schuster et al. 2019)

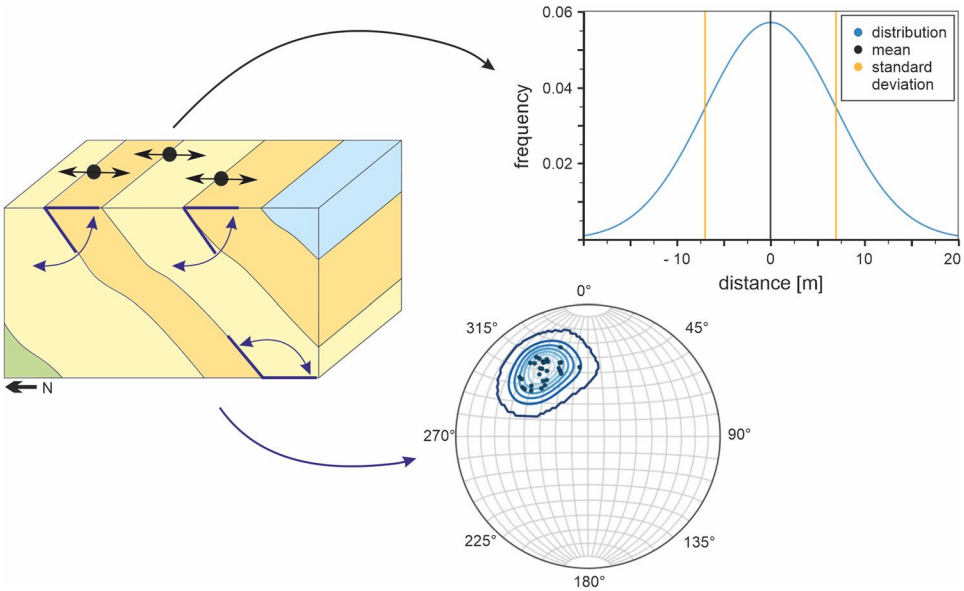

Fig. 2 Sketch of the 3D model showing the location and orientation uncertainty of the lithological contacts (color coding corresponds to Fig. 1). A normal distribution with a standard deviation of 7 m was assigned to the location of the contacts points and a von Mises–Fisher distribution with a concentration parameter of 50 was assigned to the orientation measurements

Table 1 Overview of the parameters used for the TM-coupled simulations

Bulk parameter	Shaly facies (best estimate)	Sandy facies (best estimate)
Density [kg/m^3]	2450[a]	2520[a]
Thermal conductivity (N) [Wm^{-1} K^{-1}]	1.2[a]	1.7[b]
Thermal expansion coefficient (N) [1/K]	4.2E−06[a]	1.0E−05[c]
Specific heat capacity [J kg^{-1} K^{-1}]	1155[a]	1000[c]
Poisson ratio (N) [−]	0.33[a]	0.22[a]
Young's modulus (N) [GPa]	2.8[a]	6[a]

Parameters, which are generally distinguished by anisotropy, are represented by their values normal to the bedding (N). All values for the shaly facies were obtained from Bossart et al. (2017)([a]). The density values and the mechanical rock parameters for the sandy facies were also derived from Bossart et al. (2017)([a]), whereas the thermal conductivity value was attained from Jahn et al. (2016)([b]). The thermal expansion coefficient and the specific heat capacity for the sandy facies were estimated (c)

3D model. First, a location uncertainty was allocated to the coordinates of the lithological contacts. It was assumed, that the shape of the interface itself is correct, but the location in north–south direction is uncertain. This uncertainty was defined by assigning a normal distribution to the lithological contact points, allowing the contacts of the different model realizations to shift in *x*,*y*-direction (corresponding to north–south). Based on the thicknesses of the geological layers, it was decided to use a normal distribution with standard deviation of 7 m. Furthermore, an orientation uncertainty was assigned to the orientation measurements of the lithological contacts. For this purpose, a von Mises–Fisher distribution (Pakyuz-Charrier et al. 2018) with a concentration parameter of 50 is allocated to the orientation measurements, generating a larger scatter within the orientation data (Fig. 2). With these distributions assigned to the input parameters, 89 stochastic model realizations were generated, each showing slightly different geometries with variations in layer thickness, location and strike and dip. Initially, 100 stochastic model realization was generated, of which 11 were unusable due to an incorrect geometry.

It is important to note that the choice of the geological modeling method and the parameters of the interpolation function would present additional aspects of geometrical uncertainty (e.g., Wellmann and Caumon 2018). These are not considered in this study, due to the simplified geometry, where geometrical uncertainties are mainly related to the data configuration. This is discussed more thoroughly in the "Discussion" section.

Implementing the numerical simulations in 2D

To perform 2D numerical simulations, one cross section was extracted from the initial 3D model and from each stochastic model realization. All cross sections were discretized into triangular meshes using *Triangle* (Shewchuk 1996) under consideration of the geological interface positions. The resulting meshes display an average of about 25,000 elements and 13,000 nodes. After creating the meshes, the respective rock parameters were assigned to the sandy facies 1 and 2 and shaly facies 1 and 2 (Fig. 3) according to the

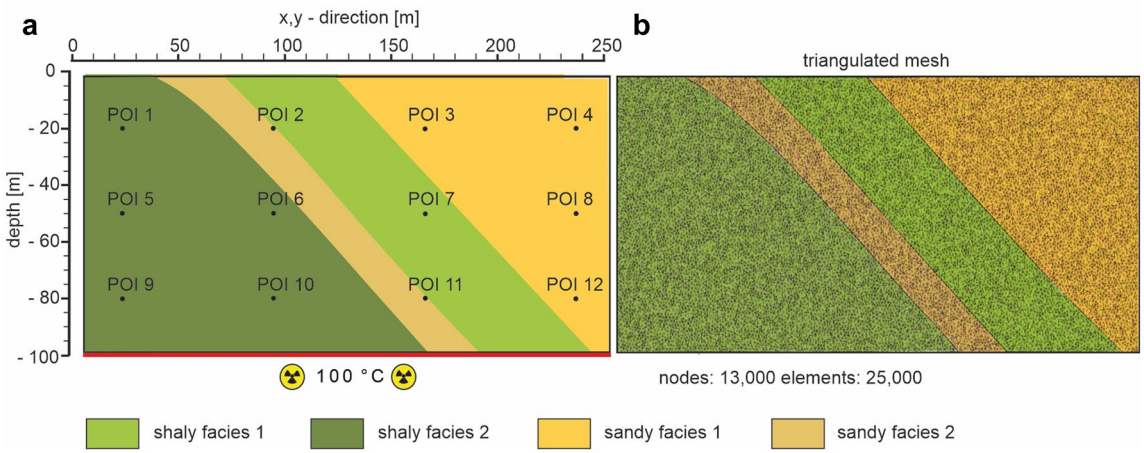

Fig. 3 **a** Cross section of the initial model showing the defined observation points and the lower thermal boundary condition, which is fixed at 100 °C. The remaining boundaries are set to zero flux. For the mechanical calculations all boundaries are fixed and equal to zero. **b** Cross section of the initial model showing the triangulated mesh.

geological model, utilizing the parameters according to Table 1.

The thermal and mechanical processes were simulated while considering the energy and momentum balance. For the energy balance, the heat transport equation without convective heat transport and without source and sink terms was taken into account (Rühaak et al. 2014; Ingebritsen et al. 2006):

$$\rho c \frac{\partial T}{\partial t} = \nabla \cdot (\lambda_T \nabla T) \tag{1}$$

where ρ is the density (kg m^{-3}), c is the specific heat capacity (J K^{-1} kg^{-1}), $\partial T/\partial t$ is the time rate of change of temperature (°C s^{-1}), λ_T is the thermal conductivity (W m^{-1} K^{-1}) and ∇T the temperature gradient (°C). The nodes at the lower model boundary were assigned a Dirichlet boundary condition, setting the initial temperature to 100 °C. This boundary condition simulates the heat source of the nuclear waste container. The temperature of 100 °C is selected since it is the maximum temperature limit defined by the German site selection act (StandAG). It should be noted that the Dirichlet boundary condition with a fixed temperature of 100 °C presents a simplification of a deep geological repository. More realistically, the heat production of the nuclear waste would decline due to the decrease in decay power (Schwenk-Ferrero 2013) and therefore the temperature would decline over time (Raiko 2012). However, with respect to study, about the impact of uncertainties in geometries, this boundary condition offers reasonable simplification. All remaining nodes are assumed to be in equilibrium and are assigned an initial temperature of 35 °C. The side boundaries were set to a Neumann boundary condition with zero flux. Considered here is furthermore a setting where a second waste gallery would be added at a regular vertical spacing and, accordingly, the top boundary condition was set equally to zero flux. For the mechanical calculations and the consideration of linear momentum balance, the linear elasticity equation was considered (Rühaak et al. 2014; Alberty et al. 2002):

$$(\lambda + \mu)\text{grad div}\,\mathbf{u} + \mu\nabla^2\mathbf{u} = -\mathbf{f} \tag{2}$$

where λ is Lamé's first parameter (−), μ is Lamé's second parameter (MPa), $\mathbf{u}$ the displacement vector and $\mathbf{f}$ the volume force. Since temperature differences are sources for stress and induce volume changes, the volume force $\mathbf{f}$ must be considered, which is denoted as following (Rühaak et al. 2014):

$$\mathbf{f} = D\beta\Delta T \tag{3}$$

All model boundaries were set to a Dirichlet boundary condition with a vectorial displacement equal to zero. This decision was made based on the deep geological location of the repository, where the load of the overburden would not allow any displacement. The simulations were then performed over a time period of 500 years, using time steps of 25 years. To obtain detailed insight into the processes during the immediate time after disposal, another simulation was run over a time period of 100 years and with time steps of 5 years.

The equations were solved with a Finite Element discretization scheme implemented in in Matlab, using a code based on Alberty et al. (1999) and Alberty et al. (2002). In addition to temperature as a simulation result, the elastic shear energy density, to display stress, and the displacement, to display strain, were calculated. The results from all TM simulations from all stochastic model realizations were compared to each other, to obtain an insight on the variability of stress, strain and temperature. Furthermore, multiple observation points were assigned to the meshes, to compare the

results of the TM simulations regarding their location within the mesh (Fig. 3).

Results

This study assesses the uncertainty of lithological contacts resulting from uncertainties in the geometric input data configuration by means of stochastic simulations. Subsequently, TM-coupled simulations were performed on the cross sections of multiple model realizations produced by the stochastic modeling process. In the following subsections, the results of the uncertainty quantification and the TM simulations will be described in detail, separately.

Uncertainties of the 3D geological model

To visualize the results of the uncertainty quantification, the uncertainties are presented by a plot of cell entropy (Fig. 4). The cell entropy is based on the Shannon entropy (Shannon 1948). The Shannon cell entropy is a common tool to represent spatial uncertainty in geological models. It is calculated based on the formation probabilities in the model cells (Wellmann and Regenauer-Lieb 2012). An entropy equal to 0 indicates no uncertainties, whereas maximum entropy reflects highest uncertainties—where uncertainties are always referring to the underlying cell outcome and are strictly limited to the validity of the geological model and the assigned parameter distributions. Figure 4 shows the cell entropy over the entire cross section. It can be observed that high cell entropies accumulate at the lithological interfaces. Further away from these contacts, the entropy reduces to a value of zero. With increasing depth, the overall entropy increases, spreading out in a cone-like manner. The maximum entropy values reach 1.5 and are observed from 50 m depth to 100 m depth where more than two outcomes are possible, between the shaly facies 2, sandy facies 2 and shaly facies 1.

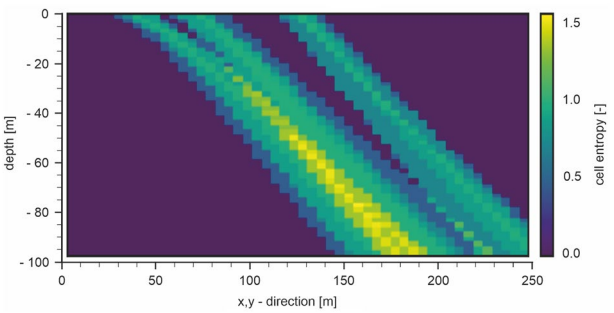

Fig. 4 Uncertainty visualized by cell entropy. Higher values of cell entropy indicate higher uncertainty

Stress, strain and temperature development in the initial model

The mean temperature of the initial model increases from 35.76 to 92.00 °C, over the simulation time of 500 years. Overall higher temperatures were noted in the sandy facies compared to the shaly facies. Furthermore, temperatures increase with proximity to the nuclear waste container (Fig. 5).

Maximum elastic shear energy density values range from 0.14 MPa to 0.28 kPa in the initial model. The stress peak is observed directly at the first time step, at 25 years after disposal. The peak is located at the interfaces of host rock and nuclear waste container (at the lower boundary of the model, see Fig. 7) and the interface of the different facies, shaly facies 2 and sandy facies 2. After the disposal, the stress decreases rapidly approaching zero. Displacement is also highest at the beginning of the simulation, decreasing with ongoing time and resulting in a mean cumulative displacement of 0.36 m after 500 years.

Comparison of all stochastic models

Reflecting the results of the stochastic models, maximum values in time of the mean temperature of all model

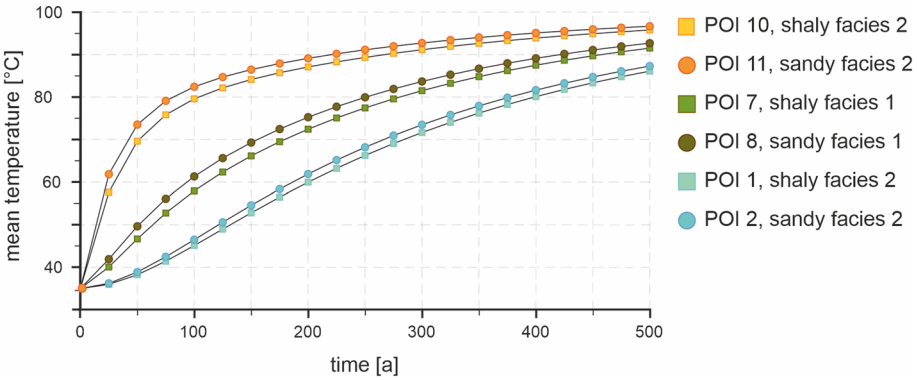

Fig. 5 Temperature development throughout different observation points within the initial model. POI 1 and 2 are the points furthest away from the nuclear waste container, whereas POI 10 and 11 are closest to the nuclear waste container. Circles represent observation points within the sandy facies and squares represent observation points within the shaly facies

realizations range between 90.89 and 92.70 °C. Mean temperatures of the model realizations deviate from the initial model by a maximum of − 1.41 °C. The deviation of mean temperature values for all model realizations at different time steps indicates that the spread of results increases with time (Fig. 6a).

Maximum values of elastic shear energy density in time and space vary between 0.02 and 0.16 MPa, with a mean value of 0.08 MPa. Maximum elastic shear energy density values of the stochastic models deviate to a maximum of 0.12 MPa to the initial model. The deviation of the maximum elastic shear energy density values for all realizations depicts that the spread of this measure decreases over time (Fig. 6b). Cumulative mean displacement values vary between 0.30 and 0.38 m. Values in displacement deviate to a maximum of 5.5 cm from the initial model.

Discussion

Uncertainties of the 3D geological model

From the uncertainty visualization (Fig. 4), it could be observed, that with increasing depth, cell entropy values increase, also covering greater areas over the whole cross section. This indicates that uncertainty in the geometric model increases with greater depth. This observation can be explained by the assigned distributions for location and orientation uncertainty. The location uncertainty, defining the position of each interface at a depth of zero, leads to only slight uncertainties at the top of the cross section. The orientation uncertainty leads to the increasing uncertainty with depth, since it increases radially into the ground. Even slight variations of the dip angle at the model surface can lead to significant variations at greater depths within the model. In conclusion, it can be said, that even though uncertainties are characterized at the surface, they are greater at depth. This is also presented in other studies, e.g., in Wellmann

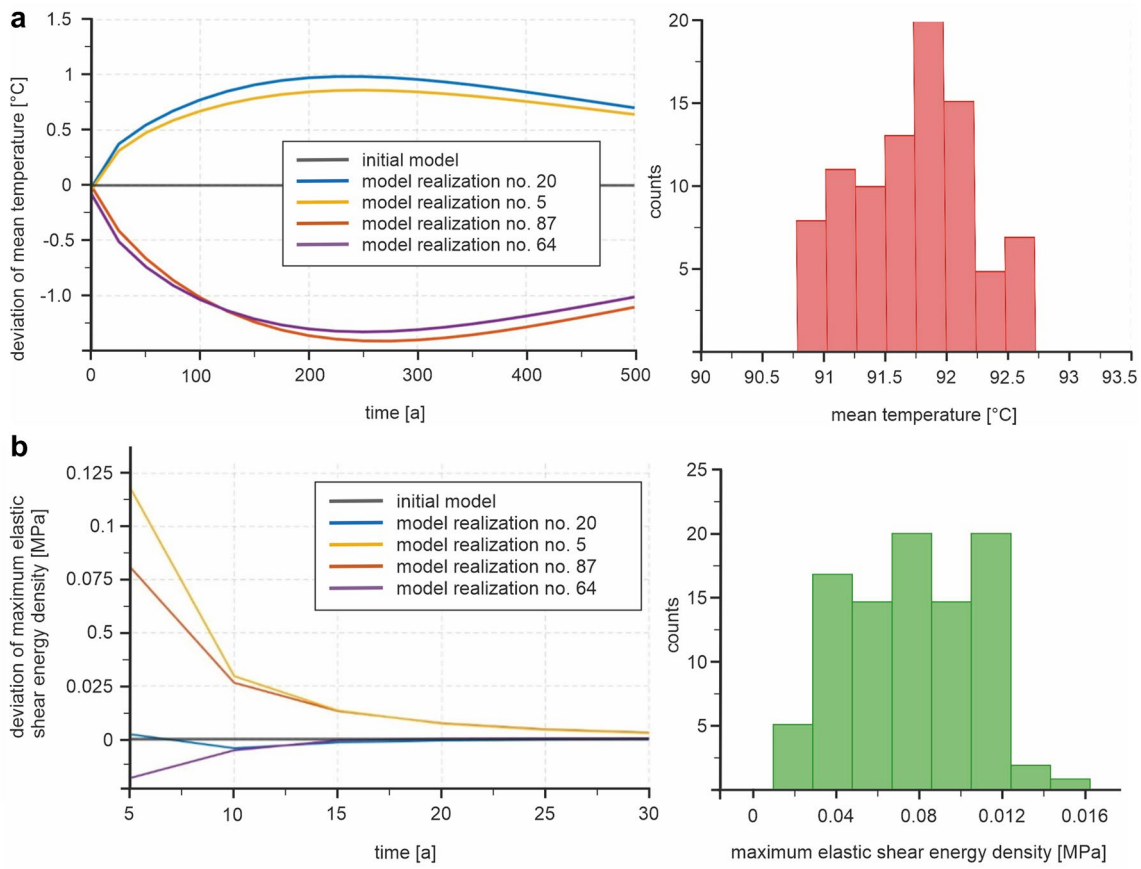

Fig. 6 **a** The *left graph* shows the maximum deviations of mean temperature from all stochastic models to the initial model. On the right, the variability of mean temperature is displayed after 500 years. **b** The *left graph* shows the maximum deviation of elastic shear energy density of all stochastic models to the initial model. On the right, the greatest variability, after 5 years, of elastic shear energy is displayed

and Regenauer-Lieb (2012). It should be noted here, that this is not a complete uncertainty quantification of the generic model. First, the exact choice the assigned distributions, as well as the parameters of these distributions, will depend on the available data type (e.g., Wellmann et al. 2010; Wellmann and Caumon 2018). Various other types of uncertainties exist, which must be taken into account for a complete uncertainty analysis. Most importantly, the geometric modeling assumption itself, characterizing property distributions in the subsurface, as well as the choice of the interpolation model and the associated parameters could be evaluated in addition to the interface data considered here (Wellmann and Caumon 2018). Still, the selected aspects of geometric uncertainty will be relevant in a realistic setting and we aim to contribute to a consideration of these uncertainties with the study presented here.

Stress, strain and temperature development in the initial model

Looking at the temperature distribution throughout the cross section, we observe that the temperature does not propagate evenly through the section and over time (Fig. 5). Higher temperatures are recorded in the sandy facies compared to the shaly facies. This results from the different thermal conductivity values of both facies. The two sandy facies have a higher thermal conductivity, presenting a value of 1.7 W m^{-1} K^{-1}. In contrast, both shaly facies present a thermal conductivity of 1.2 W m^{-1} K^{-1}. This difference results from the increased amount of quartz in the sandy facies. From this observation, it can be deduced that the temperature propagates faster in the sandy facies compared to the shaly facies. At shallower depth, the ratio of sandy facies to shaly facies increases compared to greater depth due to orientation of the formation. Therefore, an overall temperature increase in the sandy facies is more prominent at shallow depth. It should be kept in mind that the constantly increasing temperature results from the applied Dirichlet boundary condition of 100 °C. In a real-world setting, the heat production of the waste declines with time and accordingly the temperatures.

While examining the stress distribution within the cross section, it is observed that maximum stress during the first time step occurred at the model–container interface and at lithological contacts (Fig. 7). The peaks at the model–container interface can be interpreted as a result from the highest temperature difference directly at the model container interface. Peaks at lithological contacts can be explained by the temperature differences resulting from thermal rock property changes and from variations in the mechanical rock properties.

The displacement decreases with time. Again, showing that the deformation will terminate after the rock has reached the equilibrium temperature of 100 °C. The displacement presented here can be regarded as a measure to visualize the internal strain of the rock. The Dirichlet boundary conditions for the mechanical calculation represent the mechanical regime of the disposal site set 1000 m below the surface. The nuclear waste repository and the superimposed claystone are subject to the loading of the overburden. Therefore, it can be assumed, that thermal expansion is limited at this depth and internal deformation is predominant.

Comparison of all stochastic models

The variability of mean temperature values of the single model realizations is interpreted as the result from different shale–sand ratios. Due to the higher thermal conductivity of sand, higher temperatures are reached sooner in the sandy facies compared to the shaly facies. Model realizations with sandy facies showing greater thicknesses are characterized by higher mean temperatures. On the opposite, model realizations with sandy facies of smaller thicknesses and shaly facies of greater thicknesses, display lower mean temperatures (Fig. 8a, b).

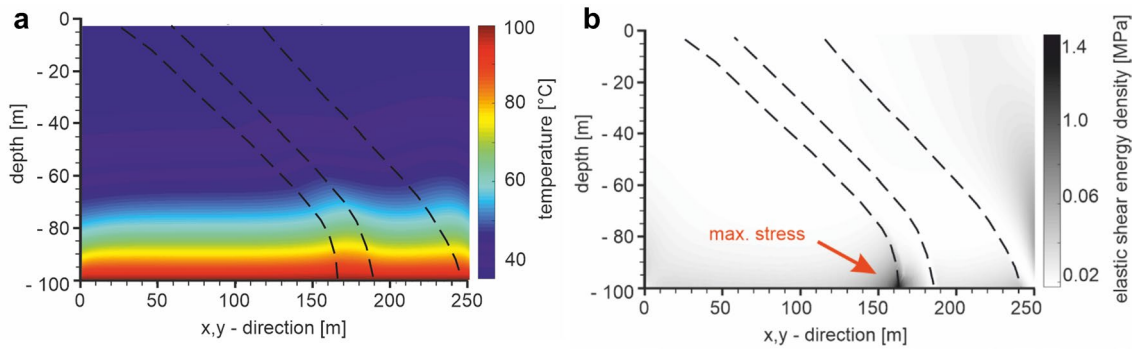

Fig. 7 Temperature (**a**) and stress development (**b**) within the initial model after the first time step (25 years). The dashed lines display the lithological contacts between the different facies. Furthermore, the location of the maximum stress is indicated in **b**

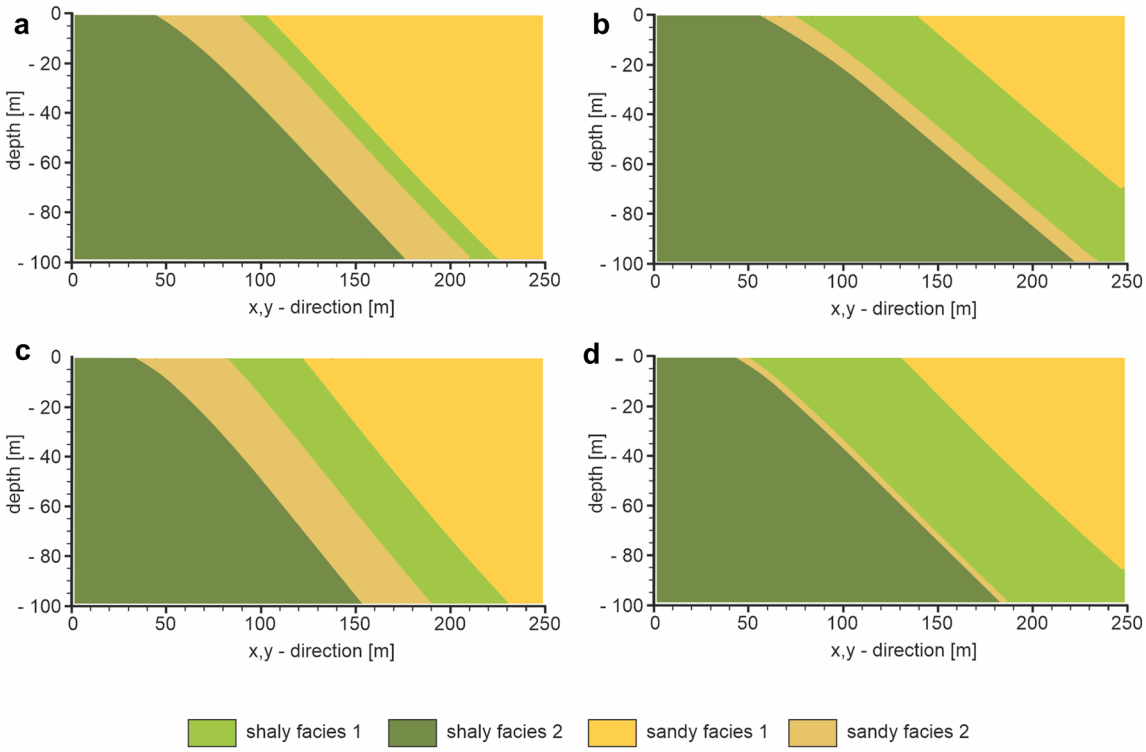

Fig. 8 Cross sections of various model realization: number 20 (**a**), which displays the highest mean temperatures and model realization; number 87 (**b**), which shows the lowest values in mean temperature. Cross sections of model realization number 99 (**c**), which displays the highest values of elastic shear energy density; and of model realization number 77 (**d**), which shows the lowest values of elastic shear energy density

Considering the results from the mechanical calculations, the greatest standard deviation of maximum elastic shear energy density was recorded directly at the first time step (Fig. 7; Fig. 6). It can be interpreted, that this variability is linked to the temperature development during the first steps. During these time steps, the temperature developments of the different model realizations depict different ascending temperature gradients. With ongoing time, the change in mean temperature decreases, approaching zero. This indicates the decreased spread of stress values over all model realizations with increase in time. As previously mentioned, the temperature differences result from the ratio of shaly to sandy facies. Therefore, it can be assumed that the thickness of the facies also correlates with the stress. Realizations with higher values show significantly thicker sandy facies compared to the realizations with lower values (Fig. 8c, d). This supports the interpretation that the stress is influenced by the geometry.

However, high temperatures do not always correlate with high stress values (Fig. 6, e.g., model no. 64, model no. 20). The model realizations of maximum and minimum temperature do not correspond to the realizations of maximum and minimum stress. Therefore, the facies thickness cannot be the only factor at play. It can be presumed that also the geometric relation and orientation of the different facies, and the simulated heat source to each other, such as the number of lithological contacts touching the lower model boundary, affect the resulting stress outcome.

Conclusion

The construction of a generic 3D model, its uncertainty analysis and subsequent 2D TM-coupled simulations allowed the assessment of temperature, stress and strain variabilities. This study provides an insight into the impact

of material contrasts and geometries associated with geological 3D models on rock integrity and on safety assessments. To study this impact, an uncertainty was assigned to all input data of the generic 3D geological model. 2D TM-coupled simulations were performed over a time period of 500 years on cross sections of different realizations of this generic model. After assigning the uncertainty to the input data, the resulting uncertainties were studied within the 2D slices. Results displayed that uncertainties increased with depth and at lithological contacts.

The results of the TM-coupled simulations present maximum mean temperature variations between 90.89 and 92.70 °C after 500 years. As explained before, these temperature values result from the applied boundary condition. However, the range of the temperature is a result of the uncertainty of the layer thicknesses of sandy and shaly facies in combination with different thermal conductivity values of each facies. Temperatures are elevated in the sandy facies and proximal to the source of heat. Furthermore, a stress variability was generated, ranging between maximum values of 0.02 and 0.16 MPa of elastic shear energy density. These variations are related to different temperature developments shortly after the model initiation and to differences in mechanical rock parameters. Peaks in stress were recorded at interfaces between facies and the simulated heat source. Mean cumulative displacements vary between maximum values of 30 and 38 cm. Maximum deviation to the initial model, the best possible model, accounts 1.4 °C of mean temperature, 0.12 MPa of maximum elastic shear energy density and 5.5 cm of mean cumulative displacement.

The observed variabilities are overall rather small. Regarding the variability of elastic shear energy density, it can be assumed that the integrity of the rock and the safety of the disposal system would not be affected. Especially taking into consideration the high confining pressures at the depth of disposal, the simulated stress in this study would not affect the host rock negatively. However, other sources of stress may add and lead to a violation of the stability criteria. To investigate this, a more detailed representation of the repository system is necessary. The physical process simulation could be extended to consider hydraulic processes or to more advanced material models, e.g., the incorporation of other parameters, such as porosity or anisotropy. An addition of stress could, for example, result from a thermally induced increase in pore pressure. Various studies exist that address this aspect by performing thermo-hydro-mechanical (THM) simulations (e.g.,Buchwald et al. 2021; Toprak et al. 2017). Likewise, THM processes, extended even further to incorporate also chemistry (THMC), are modeled and investigated by the international research collaboration DECOVALEX (Birkholzer et al. 2019).

To develop a broader and more detailed understanding of the influence of 3D geological models and uncertainties, further studies are advisable. For a more detailed consideration of uncertainties in the geological model, these studies could include, e.g., the creation of a more detailed 3D geological model, variations in uncertainty distributions assigned to the input data and their correlations, the consideration of the interpolation method itself and the spatial distribution of parameters within each geological layers, for example, using geostatistical approaches.

The model files and the code are available on request, please contact the corresponding author.

Acknowledgements Jonathan Richard Shewchuk is thanked for making Triangle openly available.

Authors' contributions M. Bjorge set up the 3D Model and carried out the simulations, made the figures and tables and wrote the first draft. P. Kreye provided technical support for Matlab. E. Heim provided technical support for GemPy and suggestions. F. Wellman supervised M. Bjorge, provided also suggestions and reviewed the manuscript. W. Rühaak came up with the overall idea, provided supervision and suggestions and reviewed the manuscript.

Funding Open Access funding enabled and organized by Projekt DEAL.

Availability of data and material Model files are available upon request from the corresponding author.

Code availability The code used is based on Alberty et al. (1999) and Alberty et al. (2002), which is openly available online.

Declarations

Conflicts of interest The authors declare that they have no competing interests.

References

Alberty J, Carstensen C, Funken SA (1999) Remarks around 50 lines of Matlab: short finite element implementation. Numer Algorithms 20:117–137

Alberty J, Carstensen C, Funken SA, Klose R (2002) Matlab implementation of the finite element method in elasticity. Computing 69:239–263. https://doi.org/10.1007/s00607-002-1459-8

BGE (2020) Zwischenbericht Teilgebiete gemäß § 13 StandAG. 28.09.2020. Bundesgesellschaft für Endlagerung mbH

Birkholzer JT, Tsang C-F, Bond AE, Hudson JA, Jing L, Stephansson O (2019) 25 years of DECOVALEX - Scientific advances and lessons learned from an international research collaboration in coupled subsurface processes. Int J Rock Mech Min Sci. https://doi.org/10.1016/j.ijrmms.2019.03.015

Bossart P, Thury M (2008) Mont Terri Rock laboratory. Project, programme 1996 to 2007 and results. Swiss Geological Survey, Wabern

Bossart P, Bernier F, Birkholzer J, Bruggeman C, Connolly P, Dewonck S, Fukaya M, Herfort M, Jensen M, Matray J-M, Mayor JC, Moeri A, Oyama T, Schuster K, Shigeta N, Vietor T, Wieczorek K (2017) Mont Terri rock laboratory, 20 years of research: introduction, site characteristics and overview of experiments. Swiss J Geosci 110:3–22. https://doi.org/10.1007/s00015-016-0236-1

Buchwald J, Kaiser S, Kolditz O, Nagel T (2021) Improved predictions of thermal fluid pressurization in hydro-thermal models based on consistent incorporation of thermo-mechanical effects in anisotropic porous media. Int J Heat Mass Transf. https://doi.org/10.1016/j.ijheatmasstransfer.2021.121127

de la Varga M, Schaaf A, Wellmann F (2019) GemPy 1.0: open-source stochastic geological modeling and inversion. Geosci Model Dev 12:1–32. https://doi.org/10.5194/gmd-12-1-2019

Ingebritsen SE, Sanford WE, Neuzil CE (2006) Groundwater in geologic processes. Cambridge University Press, Cambridge

Jahn S, Mrugalla S, Stark L (2016) Endlagerstandortmodell SÜD (AnSichT) Teil II: Zusammenstellung von Gesteinseigenschaften für den Langzeitsicherheitsnachweis. F+E Endlager Methodik und Anwendungsbezug eines Sicherheits- und Nachweiskonzeptes für ein HAW-Endlager im Tonstein. Ergebnisbericht. Bundesanstalt für Geowissenschaften und Rohstoffe Hannover

Nagra (2002) Safety Report. Demonstration of disposal feasibility for spent fuel, vitrified high-level waste and long-lived intermediate-level waste (Entsorgungsnachweis). Technical Report NTB 02–05. Nagra, Wettingen

Nagra (2014) Charakteristische Dosisintervalle und Unterlagen zur Bewertung der Barrierensysteme. SGT Etappe 2: Vorschlag weiter zu untersuchender geologischer Standortgebiete mit zughörigen Standortarealen für die Oberflächenanlage. Technischer Bericht NTB 14-03. Nationale Genossenschaft für die Lagerung radioaktiver Abfälle (Nagra), Wettingen

Pakyuz-Charrier E, Lindsay M, Ogarko V, Giraud J, Jessell M (2018) Monte Carlo simulation for uncertainty estimation on structural data in implicit 3-D geological modeling, a guide for disturbance distribution selection and parameterization. Solid Earth 2:385–402. https://doi.org/10.5194/se-9-385-2018

Raiko, H. (2012) Canister design 2012. Posiva

Rühaak W, Bense VF, Sass I (2014) 3D hydro-mechanically coupled groundwater flow modelling of Pleistocene glaciation effects. Comput Geosci 67:89–99. https://doi.org/10.1016/j.cageo.2014.03.001

Rühaak W, Heldmann C-D, Peil L, Sass I (2017) Thermo-hydro-mechanical-chemical coupled modeling of a geothermally used fractured limestone. Int J Rock Mech Min Sci 100:40–47. https://doi.org/10.1016/j.ijrmms.2017.10.019

Rühaak W, Steiner S, Welsch B, Sass I (2015) Prognosefähigkeit numerischer Erdwärmesondenmodelle. Grundwasser 20:243–251. https://doi.org/10.1007/s00767-015-0305-9

Schwenk-Ferrero A (2013) German spent nuclear fuel legacy: characteristics and high-level waste management issues. Sci Technol Nucl Install. https://doi.org/10.1155/2013/293792

Schuster K, Furche M, Shao H, Hesser J, Hertzsch J-M, Gräsle W, Rebscher D (2019) Understanding the evolution of nuclear waste repositories by performing appropriate experiments—selected investigations at Mont Terri rock laboratory. Adv Geosci 49:175–186. https://doi.org/10.5194/adgeo-49-175-2019

Shannon CE (1948) A mathematical theory of communication. Bell Syst Tech J 27(379–423):623–656

Shewchuk JR (1996) Triangle: engineering a 2D quality mesh generator and Delaunay triangulator. Appl Comput Geom towards Geom Eng 1148:203–222

SKB (2015) Safety analysis for SFR Long-term safety. Main report for the safety assessment SR-PSU. October 2015. Technical Report TR-14-01. Svensk Kärnbränslehantering AB Swedish Nuclear Fuel and Waste Management Co, Stockholm

StandAG: Standortauswahlgesetz vom 5. Mai 2017 (BGBl. I S. 1074), das zuletzt durch Artikel 1 des Gesetzes vom 7. Dezember 2020 (BGBl. I S. 2760) geändert worden ist

Toprak E, Olivella S, Pintado X (2017) Coupled THM modelling of engineered barriers for the final disposal of spent nuclear fuel isolation. Geol Soc Lond Spec Publ 1:235–251

Wellmann F, Caumon G (2018) 3-D Structural geological models: concepts, methods, and uncertainties. Adv Geophys 59:1–121. https://doi.org/10.18154/RWTH-2019-01410

Wellmann JF, Horowitz FG, Schill E, Regenauer-Lieb K (2010) Towards incorporating uncertainty of structural data in 3D geological inversion. Tectonophysics 490:141–151. https://doi.org/10.1016/j.tecto.2010.04.022

Wellmann JF, Regenauer-Lieb K (2012) Uncertainties have a meaning: Information entropy as a quality measure for 3-D geological models. Tectonophysics 526–529:207–216. https://doi.org/10.1016/j.tecto.2011.05.001